

An inter-ply friction model for thermoset based fibre metal laminate in a hot-pressing process

Liu, Shichen; Sinke, Jos; Dransfeld, Clemens

DOI

[10.1016/j.compositesb.2021.109400](https://doi.org/10.1016/j.compositesb.2021.109400)

Publication date

2021

Document Version

Final published version

Published in

Composites Part B: Engineering

Citation (APA)

Liu, S., Sinke, J., & Dransfeld, C. (2021). An inter-ply friction model for thermoset based fibre metal laminate in a hot-pressing process. *Composites Part B: Engineering*, 227, Article 109400. <https://doi.org/10.1016/j.compositesb.2021.109400>

Important note

To cite this publication, please use the final published version (if applicable). Please check the document version above.

Copyright

Other than for strictly personal use, it is not permitted to download, forward or distribute the text or part of it, without the consent of the author(s) and/or copyright holder(s), unless the work is under an open content license such as Creative Commons.

Takedown policy

Please contact us and provide details if you believe this document breaches copyrights. We will remove access to the work immediately and investigate your claim.



An inter-ply friction model for thermoset based fibre metal laminate in a hot-pressing process

Shichen Liu^{*}, Jos Sinke, Clemens Dransfeld

Faculty of Aerospace Engineering, Aerospace Manufacturing Technologies, Delft University of Technology, Delft, the Netherlands

ARTICLE INFO

Keywords:

Laminated composites
Inter-ply friction
Resin viscosity
Hot-pressing

ABSTRACT

Forming process with pre-stacked and uncured thermoset fibre metal laminate offers improved deformability compared to full-cured laminate especially for the production of complex structural components. This work investigated the friction behaviour at the metal-prepreg interface of glass fibre reinforced aluminium laminate through an inter-ply friction test. The influence of sliding velocity, normal force, fibre orientation and resin viscosity coupled with temperature on static and kinetic friction coefficients were studied. The kinetic friction behavior in the transition region between mixed and hydrodynamic lubrication, showed a good agreement with the Stribeck-curve theory. While for the static friction, a modified Coulomb friction model was found to fit the experimental results. These models were translated into a phenomenological inter-ply friction model which was incorporated into Abaqus/Explicit as a user-defined friction subroutine for verification. The findings contribute to the development of the forming process with fibre metal laminates.

1. Introduction

Fibre metal laminates are the type of lightweight composite materials made by alternating layers of fibre reinforced polymers and thin metal sheets. The hybrid structure achieves superior properties over its constituents, especially in fatigue resistance and corrosion [1,2]. For thermoset based fibre metal laminate like glass fibre reinforced aluminium laminate (GLARE), the matrix obtains its properties through a cross-linking process, also referred to as curing. This cross-linking mechanism is irreversible and usually performed in autoclaves to apply the required temperatures and pressures [3]. However, the latest development in resin pre-treatment technology has made it possible to deform fibre metal laminate with thermoset prepregs, instead of autoclaving, offering relatively short cycle times while retaining the exceptional mechanical performance as the autoclaved laminate [4,5].

Fig. 1 shows the proposed hot-pressing process of fibre metal laminate which aims at preforming an initial flat blank into the final 3D shape. The main step involves preheating the pre-stacked laminate prior to curing stage thereby decreasing the resin viscosity and increasing the ease of deformation, in particular the inter-ply friction. Temperature and time are two critical factors that need to be carefully controlled as the initiation of resin cure would increase the stiffness of the prepreg and hamper the laminate from deforming. After that, the preheated blank is

transferred to a designed mould which combines the thermoforming and curing process. The process combines sheet metal forming and composite forming methods for manufacturing the final product without losing much mechanical performance. Also, preforming an initial flat blank requires the laminate that deforms following the desired shape in a predictable and repeatable way without the occurrence of fracture, wrinkles and other possible defects [6,7]. This method is achieved by allowing the individual layers to deform by the intra-ply shear within the prepreg and inter-ply sliding in-between the metal sheets and prepreg layers.

Most of the recent papers on the frictional properties of thermoset materials are limited to unidirectional reinforcements and woven fabrics without metal layers. These studies show that processing parameters such as temperature, sliding rate and normal force greatly influence the degree of sliding deformation within and in-between the layers [8–12]. Martin et al. [13] studied the frictional resistance of woven thermoset prepreg layers and proposed that the friction coefficient depends on the prepreg system and temperature, and that prepreg with a higher viscosity and high amount of resin at the sliding surface exhibited lower frictional resistance. Akermo et al. [14] investigated the frictional properties of a unidirectional carbon/epoxy prepreg and found that fibre orientation greatly influences the friction coefficient at the prepreg-prepreg interfaces. The interfaces where 0° and 45° prepreg

^{*} Corresponding author.

E-mail address: S.Liu-7@tudelft.nl (S. Liu).

layers contact each other show the highest inter-ply friction while $0^\circ/0^\circ$ interfaces exhibit friction values similar or lower than $0^\circ/90^\circ$ interfaces. Therefore, resin rheology, fibre architecture and fibre orientation significantly influence the inter-ply friction coefficient for the thermoset polymers.

Generally, there exist two main approaches in the simulation of the forming process of composite laminates. For the micromechanical approach: all the components of composite layers are modelled including fibres and matrix. This method is supposed to be more realistic but it requires partitioning the model into small pieces, making the simulation complex and time-consuming [15]. The meso-level approach regards the composite layers as a homogeneous and continuum material which can be discretised into shell or solid elements. Usually the adhesive region between adjacent layers is simulated by using a cohesive layer with zero thickness [16,17]. This method is preferred to analyse damage problems like fracture and delamination by adopting a softening relationship between traction and separation based on cohesive law. However, these problems are less likely to occur as the inter-ply frictional force seems hard to reach the maximum normal/shear cohesive traction in the research. Besides, the three independent parameters for the cohesive model are difficult to obtain and unable to be adjusted in the applied processing conditions. Therefore, a frictional contact model applied at the interfaces can be a simple alternative method when considering relative motions of individual plies [18].

In previous frictional models for composite materials, researchers performing the forming simulation assume a constant friction coefficient at the tool-ply and ply-ply interfaces due to the lack of friction data [19, 20]. However, studies discovered that the friction coefficient greatly affects the reaction force of the tool as well as the formability and stress-strain relations on the laminate throughout the duration of the forming process. Fetfatsidis et al. [9] studied a hemisphere stamping simulation on woven fabric composites and found that the punch force is more than halved when using a friction coefficient of 0.1 versus the conventional 0.3. Mosse et al. [21] developed a finite element model for simulating the stamp forming process of thermoplastic based fibre metal laminate materials. He compared a friction coefficient of zero similar to the stamping at high temperatures where the layers can slide over each other and a very high friction coefficient of 100, corresponding to fully coupled layers at low temperatures. Results indicated that the coupled layers result in higher strains accompanied with wrinkling in a critical corner region whereas the friction-less model had a more accurate representation of the experimental surface topology and strain features. The determination of friction phenomenon plays a significant role in establishing the frictional contact model for the finite element forming simulations.

This work aims to characterise the inter-ply friction under various

sliding effects of the thermoset based fibre metal laminates like the GLARE materials. In the research, static and kinetic coefficients of friction at the metal-prepreg interface considering the influence of normal force, sliding velocity, fibre orientation and resin viscosity coupled with temperature are quantified using a designed friction-test apparatus. The two types of friction coefficient obtained from experimental results are analysed to fit the current existing friction models. Then, the process parameters for a low frictional resistance can be calculated. The study finally aims to incorporate the inter-ply friction model into a finite element simulation which could be applied in hot-pressing process.

2. Theory of friction models

Friction models between two surfaces in contact generally consist of two mechanisms. If no fluid separates the interface, the friction is governed by the force normal to the dry surface which is usually described as Coulomb friction. The Coulomb coefficient of friction can be written as [22]:

$$\mu = \frac{F}{N} \quad (1)$$

where μ is the friction coefficient, and F is the pull-out force required to overcome the normal force, N . This equation has been applied by a number of researchers in determining the effective friction coefficient of metal-fabric and metal-polymer interfaces [23–25]. However, Ajayi [26, 27] investigated the Coulomb friction effects under an isothermal condition at room temperature for cotton and wool fabrics interacting with fabric and rubber surfaces. He found that the coefficient of Coulomb friction decreased with increasing normal force while the simple linear relation between frictional resistance and normal pressure was not valid for fabrics. The effective contact surface including the types of fabric structure and the changes in yarn geometry affected the friction, while the increasing sliding velocity exhibited no consistent change in friction coefficient. Therefore, he noted that the relationship between normal force and friction force can be described as:

$$F = k \cdot N^n \quad (2)$$

where F is the friction force, N is the normal force, k and n are the frictional constant and index which can be determined from a regression analysis performed on the experimental data.

Besides the Coulomb friction which occurs between dry surfaces, purely hydrodynamic friction exists when two surfaces in relative motion are completely separated by a fluid film. In this case the friction can be predicted in terms of the traction force acting on the film, ignoring the effect of surface roughness on the friction [28]. The hydrodynamic friction is independent of the normal force under steady load conditions,

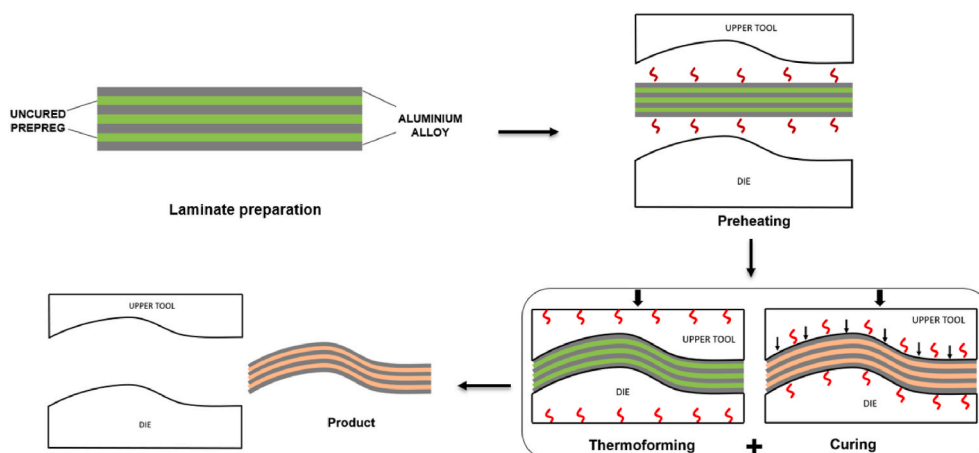


Fig. 1. Proposed hot-pressing process of fibre metal laminate manufacturing.

but depending on resin viscosity and shear rate as shown:

$$\tau = \eta \cdot \dot{\gamma} \quad (3)$$

where τ is the shear stress, η is the viscosity of the matrix, $\dot{\gamma}$ is the shear rate. In addition to the two friction mechanisms, Wilks [29] designed a pull-out test that uses springs to apply normal pressure and pulls a thin metal sheet from two platens covered with a pre-consolidated fibre-glass-polypropylene fabric. He analysed the effect of processing parameters on shear stress τ and established a friction model accounting for the effect of both Coulomb friction and hydrodynamic friction as shown:

$$\tau = \mu \cdot PN + \eta \cdot \dot{\gamma} \quad (4)$$

where μ is the Coulomb friction coefficient, P is the normal pressure, η is the viscosity and $\dot{\gamma}$ is the shear rate. Based on the experiments, he found that the shear rate had the largest effect on the shear stress, followed by normal pressure and viscosity influenced by temperature.

Clifford [30] optimised the Wilks' friction model by adding a term for the effective contact ratio on Coulomb friction by investigating tool-ply friction interaction for thermoplastic composite sheet between two steel plates. His analytical model considered both Coulomb friction and experimentally obtained viscous resistance of the polymer film due to the variation in shear stress with pull-out rate and temperature,

$$\tau = \varphi \cdot \mu \cdot PN + \eta \cdot \dot{\gamma} \quad (5)$$

where φ is the ratio of dry fibre regions in effective contact to the whole mould surfaces. The models showed good agreement with experimental results for shear stresses larger than 0.02 MPa.

Stribeck developed a theory to describe various types of friction mechanisms in relation to sliding velocity, bearing pressure and lubricant viscosity in tribology [31,32]. He identified that at low sliding velocities, surface asperities coming into contact dominate and lead to high friction coefficients (called boundary lubrication), whereas at high velocities the normal pressure is dominated by hydrodynamic pressure resulting in low friction coefficients (called hydrodynamic friction). The so called Stribeck-curve which plots the relation of friction coefficient versus Hersey number shown in Fig. 2, exhibits the characteristic transition region between boundary, mixed and hydrodynamic lubrication. The Hersey number H , also referred as the Stribeck number, can be interpreted as a normalised sliding velocity as a function of matrix viscosity, η , sliding velocity, ν , and normal force, N ,

$$H = \frac{\eta \cdot \nu}{N} \quad (6)$$

Fig. 2 demonstrates a theoretical Stribeck curve and shows the three lubrication regimes based on the type of friction mechanisms. The first region is governed by boundary lubrication where the fluid film is negligible resulting in the friction similar to Coulomb friction. The

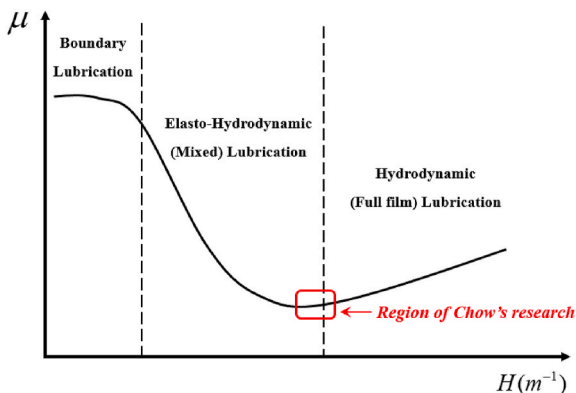


Fig. 2. Stribeck curve on friction coefficient versus Hersey number, indicating the range of Chow's research [25].

second part is an elasto-hydrodynamic mode friction, which is also referred as mixed lubrication. This mode would gradually transfer into a third hydrodynamic (full-film) region when the lubrication layer becomes thicker. The surfaces in this area are completely separated by a fluid film and the friction coefficient increases as the lubrication layer thickness increases. The curve provides a qualitative explanation of the mechanism influencing the friction coefficient for a range of processing parameters such as normal force, sliding rate, resin viscosity and temperature. This theory has been applied to study the friction at the interfaces of different composite laminates as well as the tool-ply interactions [9,12,33]. Chow [25] proposed an analytical model for friction behaviour of a glass-polypropylene woven fabric between the forming binder and die from the test results. He predicted the effective friction coefficient that can be used in numerical simulations under different processing values by incorporating weighted effects of Coulomb and hydrodynamic friction models. The results demonstrated the transition between these two friction mechanisms for various combinations of experimental parameters fitted to a corresponding relationship of the Stribeck curve.

The combination of normal force and sliding velocity in Eq. (6) can be adjusted to obtain equal Hersey numbers at a constant viscosity. Consequently, the friction coefficients are expected to be equal in a particular surface interaction with equal Hersey numbers. As polymer viscosity is dependent on the processing history, a rheological model needs to be established for the calculation of Hersey numbers. At a given temperature, the viscosity for thermosets evolves as a function of the degree of cure. The empirical formula for temperature and degree of cure dependent viscosity model of the thermoset matrices can be expressed as [34,35]:

$$\eta = \eta_{\infty} \exp\left(\frac{\Delta E \eta}{RT} + kac\right) \quad (7)$$

where η_{∞} is the initial viscosity, $\Delta E \eta$ is the viscous activation energy, k is a constant, R is the universal gas constant and T is the absolute temperature in Kelvin. Once the test temperature and degree of cure for a certain epoxy thermoset is determined, the viscosity can be obtained using the rheological equation. Then, the relationship between friction coefficient and Hersey number considering viscosity and temperature effects can be discussed further in section 5 of the paper.

3. Experiment

3.1. Material

The material systems used in this study are the aerospace graded fibre metal laminates named as GLARE which are glass fibre reinforced aluminium laminates. The experimental samples were made of three 0.5-mm thick 2024-T3 aluminium sheets and two layers of glass fibre reinforced unidirectional prepreg S2-glass/FM-94 epoxy. Each glass fibre layer included two prepreg plies and the nominal thickness was 0.18 mm for each ply. The unidirectional fibre oriented at 0° direction corresponded with the rolling direction of the aluminium sheet. Prior to assembling, the aluminium surfaces were pre-treated with chromic acid anodising and primed with BR 127 for corrosion inhibiting [36–39] because the surface treatment has a great influence on the friction studied in the research. Conventional manufacturing process for GLARE materials was through standard autoclave cycle with 1-h curing at a maximum temperature of 121°C and an autoclave pressure of 6 bar. In this research, the laminate samples were pre-stacked and pre-heated following the cycles shown in Fig. 3. The specimen underwent an initial heating rate of $5^{\circ}\text{C}/\text{min}$ to the target temperature and subsequent holding to a constant time of 20 min. The layup configuration and thickness of pre-stacked laminates in the research are presented in Table 1.

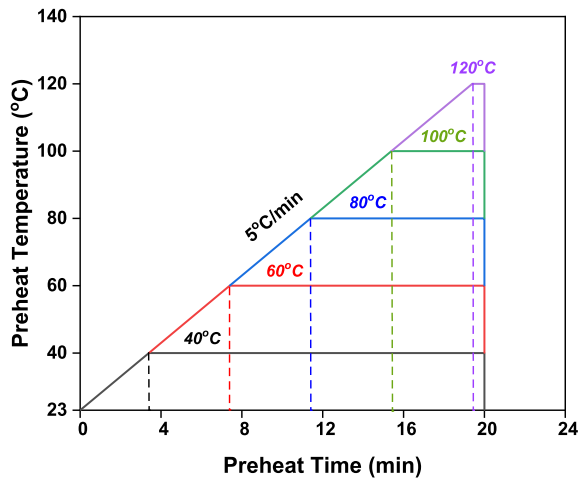


Fig. 3. Preheat temperature and time cycles for the pre-stacked GLARE materials.

3.2. Setup

Current friction measuring methods consider the effects of normal force, pull-out velocity and temperature, while other factors which are critical in composite forming process such as resin viscosity and fibre orientation have not been taken into account [22–25]. Modifying the ASTM standard D 3528 [40] which is used to determine the tensile shear strengths of adhesives for bonded metals, an inter-ply friction test apparatus based on a double lap specimen which allowed for testing at various conditions, was designed for the measurement of the friction coefficient at the metal-prepreg interface. Instead of bonding and curing through standard autoclave cycle, the outer prepreg layers could slide along the pre-treated aluminium sheets and the inner layers may slide relative to one another under specified normal loads. The heated resin was not only the matrix material of the resulting prepreg but also acted as a lubricant as the prepreg slides between two metal plates. The sliding friction had been shown to follow the Stribeck-curve hypothesis as stated in section 2, where hydrodynamic lubrication assumed the contacting surfaces were fully separated by a fluid film and elasto-hydrodynamic lubrication accounted for the deformation of the surfaces.

The schematic diagram and dimension for the laminate sample was presented in Fig. 4 and a normal force was applied on top and bottom aluminium sheets by a clamping loadcell ($40 \times 40 \text{ mm}^2$) using fine thread locking screws as shown in Fig. 4(c). The force was measured by strain gauges in a wheatstone bridge, which were installed on the central region of the clamping loadcell. Fig. 5 (a) exhibits the calibration test of the normal force and the result shown in Fig. 6 was used as the reference values for different test temperatures. The apparatus was used in a Zwick-20kN tensile/compression machine with a temperature chamber. The samples were put into the tensile machine and clamped by the loadcell in normal direction shown in Fig. 5 (b). The loadcell along the pull-out direction was fixed by a rope and the normal force can be adjusted to selected values through the rotating shaft. The temperature inside the chamber can be preset and read by a thermocouple in contact with the aluminium sheet. Other variables such as fibre orientation and sliding velocity can be altered by layup design and manual input.

The load-displacement relationships under different conditions were

Table 1
Details of layup configuration and thickness of pre-stacked laminates.

Structure	Stacking configuration	Total Thickness
GLARE 3/2	Al/[0/0]/Al/[0/0]/Al Al/[45/45]/Al/[45/45]/Al Al/[90/90]/Al/[90/90]/Al	2.22 mm

measured up to a pull-out displacement of 20 mm. Because the clamping apparatus has two friction surfaces in contact with the top and bottom aluminium sheets, a factor of two is included in the denominator of Coulomb's Law to obtain the experimental coefficient of friction as,

$$\mu = \frac{F}{2 \cdot N} \quad (8)$$

where F is the pull-out force obtained from the experiments and N is the set value of the normal force applied by the clamping loadcell. The friction coefficient calculated from Eq. (8) was extracted from test data until the normal force begins to drop, and at least three samples were tested for each test configuration.

To investigate the influences of different parameters on the friction coefficient at the metal-prepreg interfaces, a set of value ranges were chosen for these parameters. Experiments were conducted varying one or two parameters at a time while keeping all other parameters at their baseline value. Table 2 lists the parameters investigated for the friction test. These selected parameters were designed to show whether the relationship between the friction coefficient and Hersey number followed the trend of a Stribeck curve. Equal Hersey numbers determined through various normal force and sliding velocity combinations should result in equal friction coefficients. Therefore, two sets of test parameters were selected for each of the nine Hersey numbers (Table 3) where the constant viscosity (η_0) for the experimental prepreg was assumed to be around 10^4 Pa s at room temperature (23°C) [41].

For the fibre-reinforced epoxy FM-94 applied in the experiment, the viscosity was mainly influenced by the temperature and degree of cure. According to Eq. (7), three modelling parameters should be determined and applied in the viscosity model. From prior research and model fitting procedure [42–44], the rheokinetic model constants for FM-94 epoxy in Eq. (7) are given in Table 4. Fig. 7 reveals the predicted cure development of the FM-94 epoxy at different test temperatures including the degree of cure as a function of time and the viscosity evolutions. In this research, inter-ply friction experiments on pre-stacked fibre metal laminate were conducted at the preheat temperature of 40, 60, 80, 100, 120 °C and those temperatures were kept constant for the entire preheat period. Because the whole process consists of an initial heating ramp and subsequent holding at the preheat temperature, the viscosity was calculated at the final stage of preheating. Viscosity values used in the friction model with a constant preheat time of 20 min are calculated by Eq. (7) shown in Table 5. Incorporating the viscosity parameters into Hersey number (Eq. (6)), the relationship between the friction coefficient and Hersey number at various temperatures can be obtained to see if they fit the Stribeck curve.

4. Results and discussion

All the results for the pull-out force and displacement relationship follow the same general trend shown in Fig. 7. Firstly, the laminate samples experience elastic deformation where the pull-out force increases sharply and reach a peak without movements at the metal-prepreg interfaces. This force corresponds to the static friction force required to initiate sliding between surfaces. After that, the load drops quickly and reaches a steady sliding corresponding to kinetic friction. This kind of stick-slide phenomenon could be analogous to the Stribeck-curve theory, where the interfaces overcome a boundary condition with high friction, break surface asperities and establish a lubrication layer that leads to the occurrence of kinetic sliding. In Fig. 8, point A

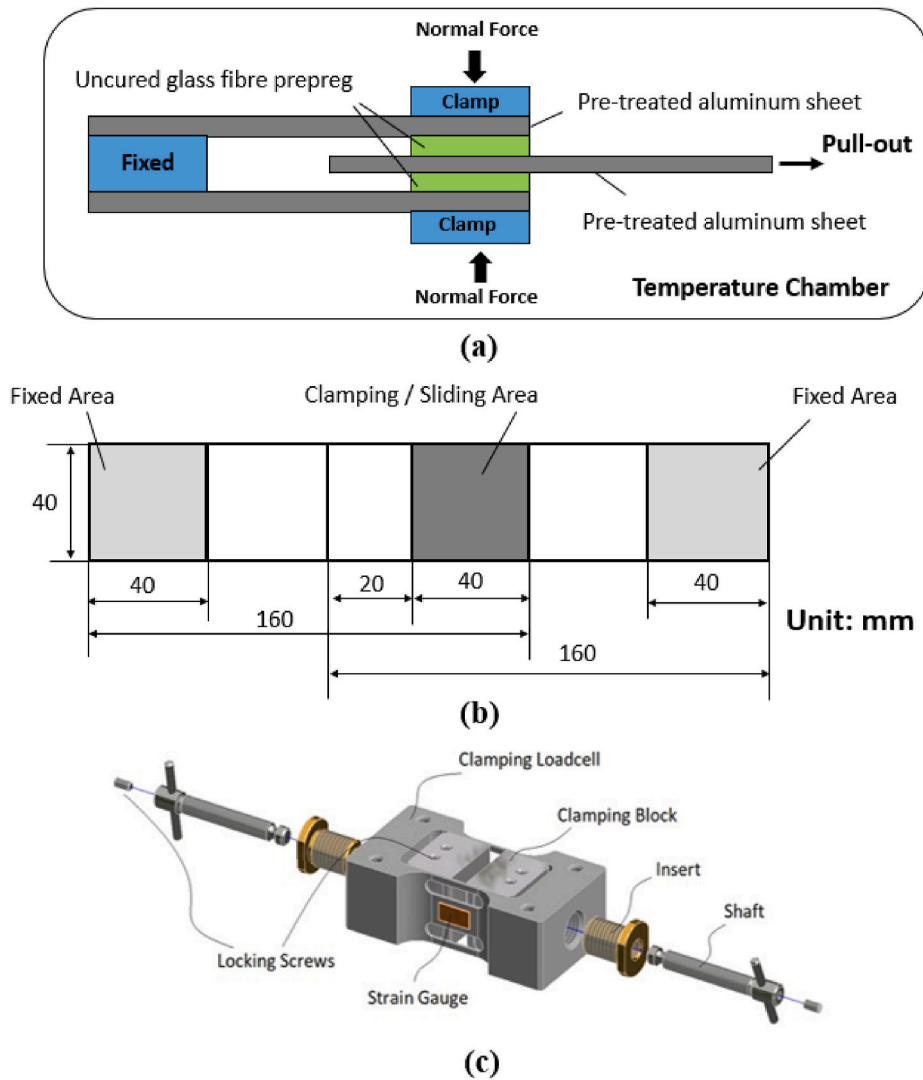


Fig. 4. (a)Schematic diagram and (b) Dimension for the inter-ply friction test, (c) Details of the clamping loadcell unit.

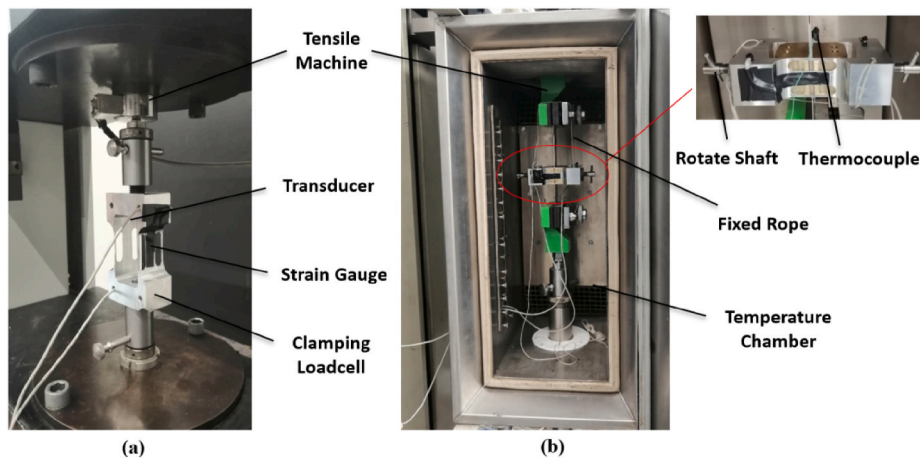


Fig. 5. Experimental setup and apparatus: (a) Calibration test of the normal force; (b) Inter-ply friction test.

represents the initial static peak force, and the displacement was calculated to be less than 0.5 mm. The displacement at point B for steady sliding was assumed to be 10 mm for all test configurations as the normal force gradually drops after that in the experiment. The pull-out

forces at point A and B were used in Eq. (8) to calculate the values for the static and kinetic friction coefficients, respectively. Based on the obtained experimental results, an investigation considering different sliding parameters on the friction coefficient and the initial fitting of the

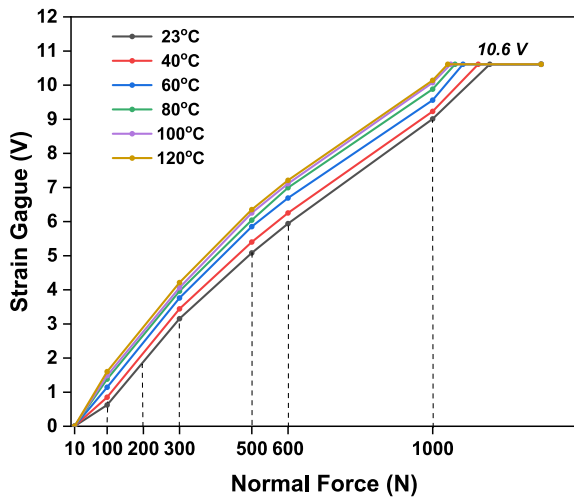


Fig. 6. Normal force and strain voltage curve under various temperatures for the clamping loadcell.

Table 2

Test parameters used for inter-ply friction experiments.

Parameter	Baseline value	Additional values investigated
Normal force (N)	500	100, 200, 300, 600, 1000
Sliding velocity (mm/min)	10	5, 15, 20, 30, 40
Fibre orientation (°)	0/0	45/45, 90/90
Preheat temperature (°C)	23	40, 60, 80, 100, 120

Table 3

Test conditions for Hersey number studied at room temperature ($\eta_0 \approx 10^4 \text{ Pa} \cdot \text{s}$).

Test	Hersey number (m^{-1})	Velocity (mm/min)	Normal force (N)
A-1	1.67E-3	5	500
A-2	1.67E-3	10	1000
B-1	2.78E-3	5	300
B-2	2.78E-3	10	600
C-1	3.33E-3	10	500
C-2	3.33E-3	20	1000
D-1	4.17E-3	5	200
D-2	4.17E-3	15	600
E-1	5.0E-3	15	500
E-2	5.0E-3	30	1000
F-1	6.67E-3	20	500
F-2	6.67E-3	40	1000
G-1	8.33E-3	5	100
G-2	8.33E-3	15	300
H-1	1.67E-2	10	100
H-2	1.67E-2	30	300
I-1	3.33E-2	20	100
I-2	3.33E-2	40	200

Table 4

The constants used in the viscosity model (Eq. (7)) for FM-94 epoxy [39–42].

η_∞ (Pa·s)	$\Delta E\eta$ (kJ/mol)	k
3.38E-3	36.67	10.44

Stribeck curve for the inter-ply friction model was considered.

4.1. Effect of normal force and sliding velocity

Fig. 9 shows the experimental results of the static and kinetic friction coefficients and illustrates the influence of normal force on the inter-ply friction tested at various sliding velocities. For the test values in the figure, two other factors, the fibre oriented at $0^\circ/0^\circ$ and the room

temperature of 23°C , were kept at the baseline values. It can be seen that both the static and kinetic friction coefficients increase with the increasing sliding velocity and this relationship suggests that friction is characterised by Newtonian shearing of the epoxy matrix where shear stresses increase with the increasing shear rate. In contrast, the friction coefficient decreases with the increasing normal force and the kinetic friction drops before reaching a minimum value and plateau. One explanation is that for low normal forces, interfaces between fibre reinforced prepreg and pre-treated aluminium sheet have a relatively rough surface contact with high asperities. Although higher frictional forces are required to pull the adjacent surfaces apart as the normal force increases, the oriented fibres as well as asperities at the contacting interfaces can be flattened out, resulting in a reduction of the roughness and consequently, the friction coefficients. The sketch of this phenomenon is illustrated in Fig. 10 and upon increasing the normal force, further compaction of the laminate seems impossible because the frictional force would greatly increase and even damage may occur when the fibres in prepreg have direct contact with the aluminium surface.

Cross-section Micrographs of the sample perpendicular to the sliding direction after the friction test (Fig. 11(a)) are shown in Fig. 12. The samples are tested with a normal force of 200 and 1000 N at the temperature of 80°C . Two fibre reinforced composite layers are separated by three aluminium sheets shown in white regions and the interfaces can be perfectly discerned. The thicknesses of each prepreg are varied after the friction test because of the different intraply viscous effects at specified conditions and four values at different areas are measured to obtain an average thickness. The thicknesses measured on the micrographs showed that a normal force of 1000 N leads to a higher degree of compaction compared with a lower normal force of 200 N. The nominal thickness for each prepreg layer is $360\ \mu\text{m}$. The average thickness after performing the friction test with a normal force of 200 N is $292.3\ \mu\text{m}$, while it is calculated to be $270.9\ \mu\text{m}$ on average with a normal force of 1000 N. It can be concluded that the thickness decreases with the normal force increases and that thickness reduction leads to a lower friction coefficient.

The tests conducted to examine the effect of normal force and sliding velocity on the friction coefficient are presented to determine the applicability of the Stribeck curve for this research. The results in Fig. 13 are plotted with the average experimental results for the inter-ply friction samples. Upon fitting these experimental results, it is determined that the Hersey numbers investigated at room temperature for kinetic friction coefficient look to fall into the hydrodynamic lubrication region in the Stribeck curve (Fig. 2), as the region appears exponential and has a positive slope similar to the trend indicated by the experimental results (Fig. 13(a)). It is observed that equal Hersey numbers do obtain equal friction coefficient within the standard deviation and the kinetic friction values gradually stabilise as the Hersey number gets smaller. For the static friction coefficient curve plotted in Fig. 13 (b), the trend follows a power law which does not correspond to the Stribeck curve and therefore cannot be explained with the known concept of fluid lubricated contacts.

4.2. Effect of fibre orientation

Orientation of the unidirectional fibres within the prepreg varies during the forming process, and the potential effect for different fibre orientation such as $0^\circ/0^\circ$, $45^\circ/45^\circ$ and $90^\circ/90^\circ$ on friction was investigated. The results showed that fibre orientation did not affect the coefficients of static friction. This outcome is mainly due to the fact that the fibre orientation in the prepreg has little impact on the fibre asperities and initial degree of intimate contacts, which mostly decide the evolution of static friction. However, the kinetic friction behaves differently under various conditions of normal force and temperature. Fig. 14 exhibits the experimental results of these two sliding effects in three different fibre orientations and the other variables are kept at their baseline values. It is shown that the kinetic friction coefficient decreases

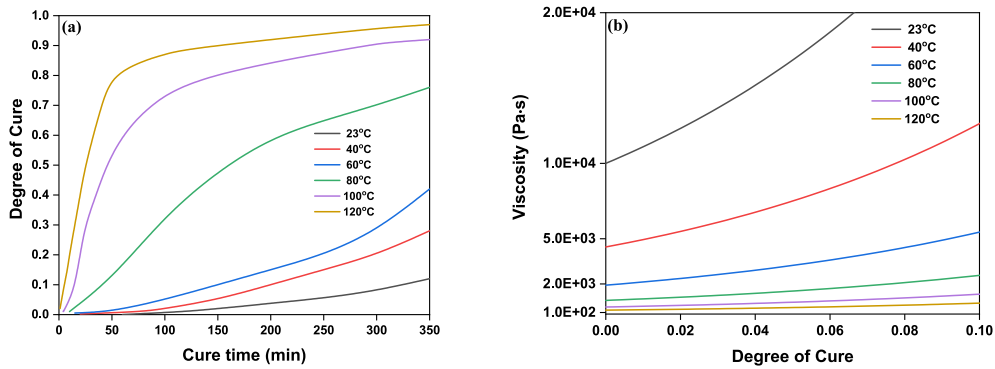


Fig. 7. Predicted cure development of FM-94 epoxy at different test temperatures:(a) Degree of cure; (b) Viscosity.

Table 5

Computed viscosity used in the friction models with a constant preheat time of 20 min.

Temperature (°C)	Degree of cure	Viscosity (Pa·s)
23	0	9997.8
40	0.001	4501.3
60	0.004	1993.1
80	0.008	981.5
100	0.011	518.3
120	0.016	299.2

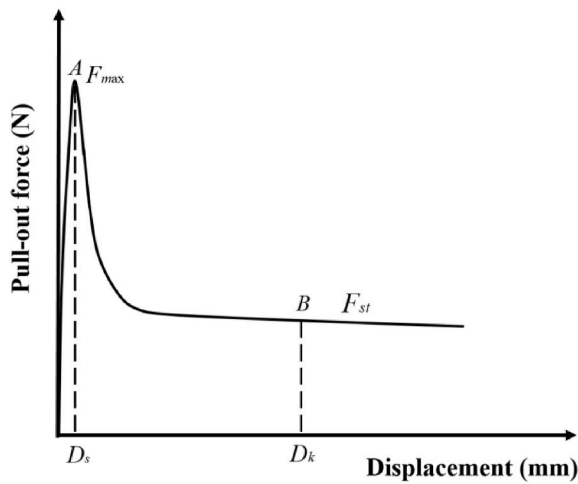


Fig. 8. Schematic curve of pull-out force and displacement relation for the friction test.

as the normal force or temperature increases. The fibre oriented at 45°/45° exhibits the highest kinetic friction coefficient while the 0°/0° layup interfaces show a lower friction coefficient compared with 90°/90° interfaces under the same conditions. The difference implies that the presence of 45° and 90° plies increase interfacial shear stress because of the interlocking phenomenon when fibre orientation and aluminium rolling direction deviates. The effects of fibre orientation become more distinct with the increase of temperature, which suggests that the interactions at the metal-prepreg interfaces occur by the direct contact between the oriented fibres and aluminium surface at elevated temperatures.

The trend can be further explained through investigation of micrographs of the sliding surface and cut-outs. Sliding surfaces are performed by a digital microscope to recognize the variations of sliding length in Fig. 11(b). The fibre orientation of 45°/45° and 90°/90° at room temperature coupled with the temperature at 80 °C after the inter-ply

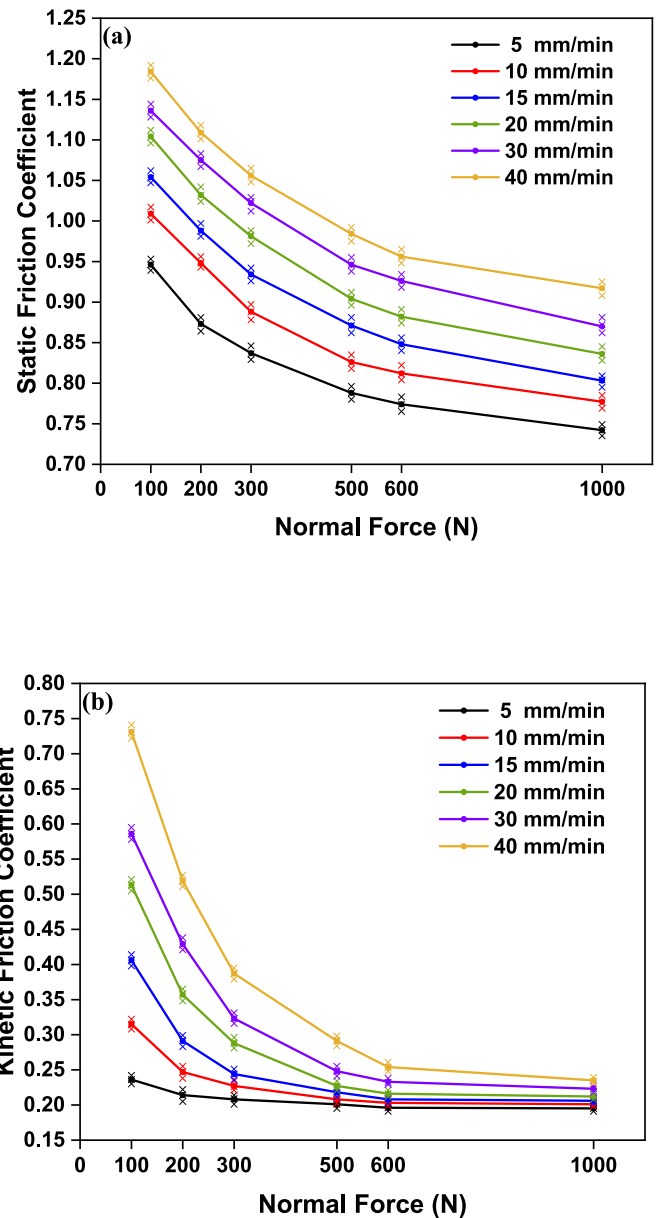


Fig. 9. Friction coefficients as a function of normal force and sliding velocity at room temperature: (a) Static; (b) Kinetic.

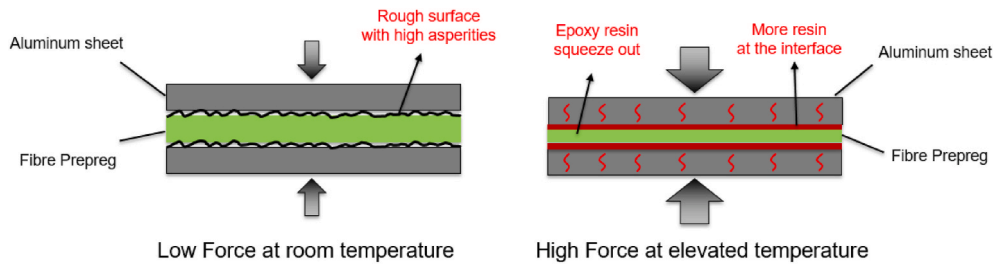


Fig. 10. Sketch for illustrating the effect of normal force and temperature after the friction test.

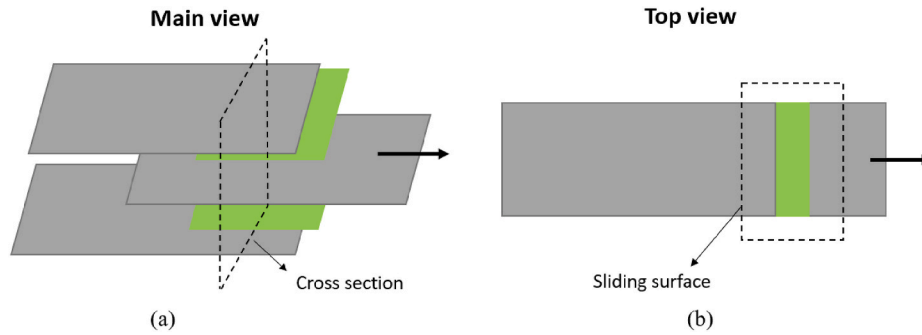


Fig. 11. Sketch of the laminate sample after the friction test: (a) Cut-outs; (b) Sliding surfaces.

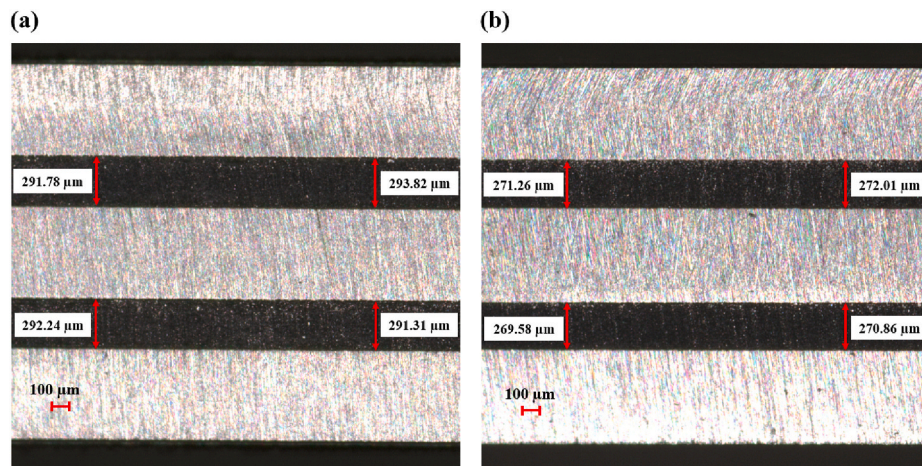


Fig. 12. Cross-section micrographs after friction test performed with a normal force of (a): 200 N and (b)1000 N at the temperature of 80 °C – (× 80).

friction test are shown in Fig. 15. A corresponding pull-out of fibre reinforced preregs can be observed with the movement of middle aluminium sheet. At room temperature, the average sliding length for the 45°/45° layup prepreg is 6.22 mm and the value increases to average 6.75 mm with the orientation of 90°/90°. The increase in prepreg sliding length means a lower frictional resistance at the interface. Even though the maximum displacement for both layups shows a positive elevation at high temperature, the laminate with 45°/45° interfaces exhibits a decrease in sliding length of prepreg on the bottom side. This phenomenon can be explained by the occurrence of intra-ply shear for 45°/45° interfaces while layups of 0°/0° and 90°/90° only undergo inter-ply sliding during the friction test. The inter-ply sliding dominates the evolution of friction coefficient while intra-ply shear within the prepreg also contributes to friction. Therefore, the 45°/45° interfaces have the highest kinetic friction coefficient values compared with the 0°/0° and 90°/90° interfaces. In addition, the shearing phenomenon at elevated temperature demonstrates that decreasing viscosity has a positive influence on both inter-ply sliding and intra-ply shear behaviours. Fig. 16

shows that the cross-section thickness slightly drops from for 45°/45° interfaces to 90°/90° interfaces at the temperature of 80 °C. This small difference of thickness shows that the fibre-orientation effect has a limited influence on the thickness reduction and friction coefficient. Although it affects the kinetic friction coefficient at various normal forces and temperatures, it is not a factor in the determination of the Hersey number using Stribeck-curve theory or other friction models and no consistent law can be followed. Therefore, fibre orientation was not further considered for the development of the inter-ply friction model in this paper.

4.3. Effect of resin viscosity and temperature

To investigate the influence of resin viscosity on friction coefficient, the combinations of the sliding velocity and normal force (v/N) are kept constant ranging from 0.01 to 0.1 mm/N·min shown in Fig. 17. In this research, the resin viscosity decreases with the elevation of test temperature. Results reveal that the static and kinetic friction coefficients

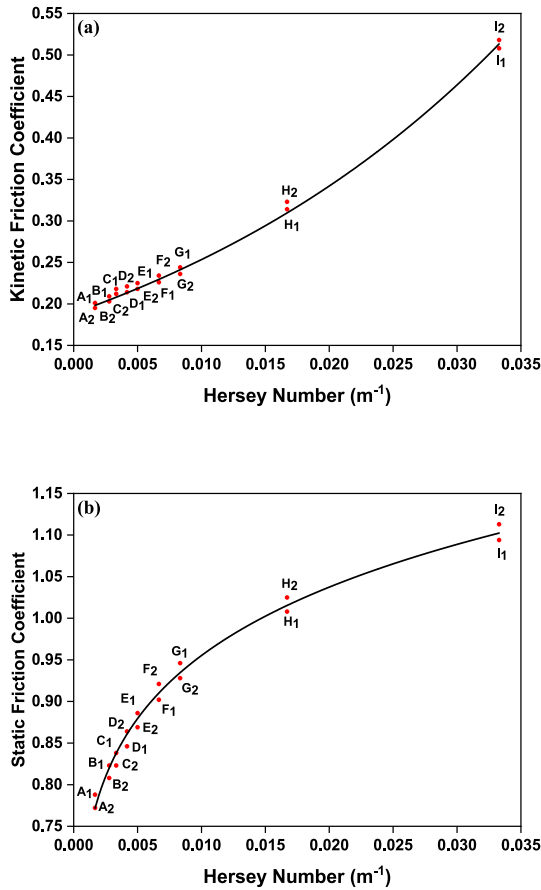


Fig. 13. Hersey number versus experimental friction coefficient at room temperature: (a) Kinetic; (b) Static.

decrease as the test temperature increases from the room temperature of 23 °C to the maximum temperature of 120 °C. Rather than the quasi-linear reduction of static friction as the test temperature increases, the kinetic friction coefficient gradually converges at elevated temperatures. It can be concluded from the results that an increase of resin flow as viscosity decreases has a significant influence on the friction. The decreasing trend in the friction coefficient can be due to the resin squeezing out from the center of prepreg layer to the top and bottom interfaces. More resin at the interfaces creates resin film layers which increase the lubrication and reduce the friction coefficient as discussed in the Stribeck-curve theory. The illustrating sketch is also shown in Fig. 10. However, the viscosity variations provide limited effects on the static friction state before the onset of sliding, and the decrease in friction coefficient may result from the temperature effect which alters the interface asperities. In addition, the combined effect of sliding velocity and normal force has a small influence on the kinetic friction coefficient as the temperature rises.

Fig. 18 shows the micrographs of the sliding surfaces at three different temperatures while all other parameters are kept at their baseline values. A slight increase for the sliding length of prepreg layer shown on the surface top region are measured from 7.05 mm at 40 °C to 7.62 mm at 120 °C. This result helps to explain why the friction coefficient drops with increased resin flow by the elevation of test temperatures. However, it is also obvious to see the uneven ply boundary displacement on the surface bottom region for 0°/0° interfaces at the temperature of 120 °C in Fig. 18. There are two reasons which can explain the defects: One is that the polymer matrix tends to flow parallel to the fibre axis, which makes the transverse flow less likely to happen.

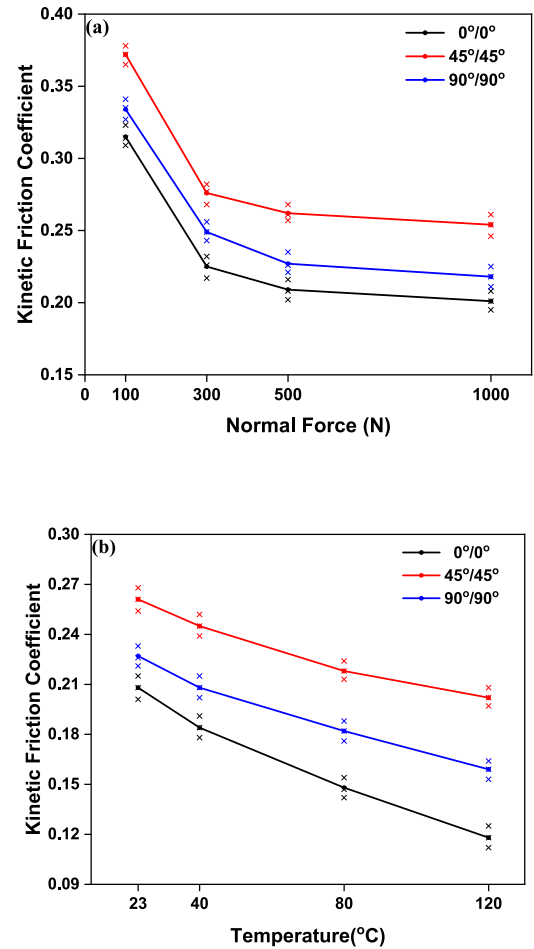


Fig. 14. Kinetic friction coefficients of normal force at room temperature of (a) 23 °C and temperature at (b) 500 N.

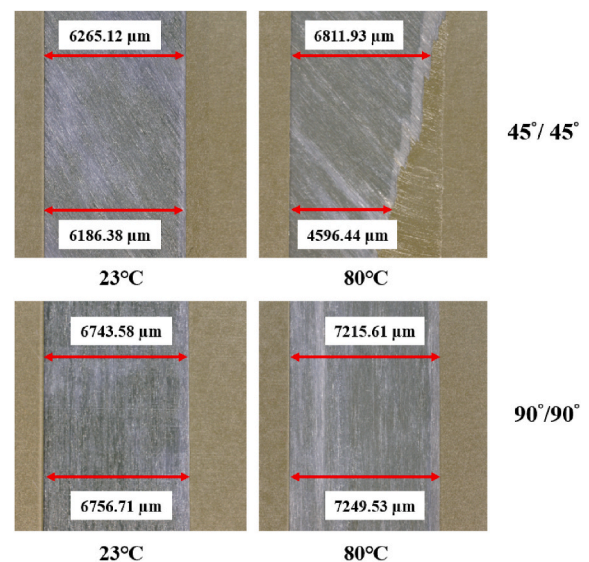


Fig. 15. Sliding surfaces after the friction test performed with different fibre orientations - (× 12).

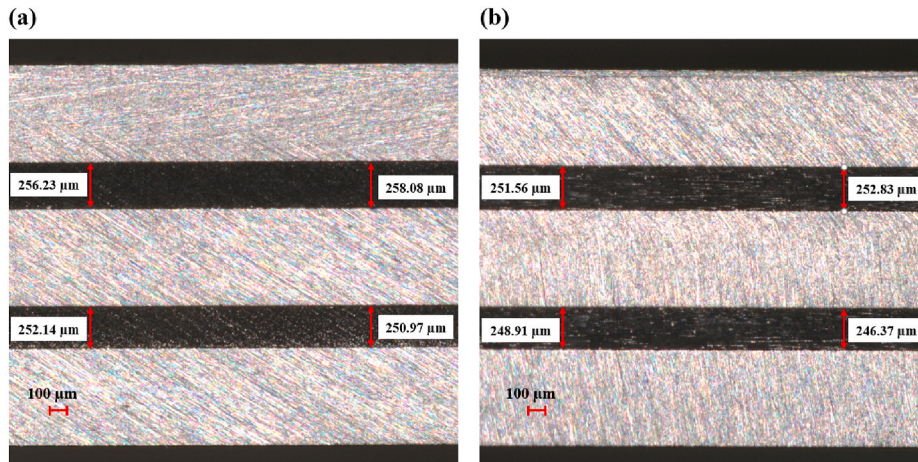


Fig. 16. Cross-section micrographs after friction test performed with a fibre orientation of (a) 45°/45° and (b) 90°/90° at the temperature of 80 °C – (× 80).

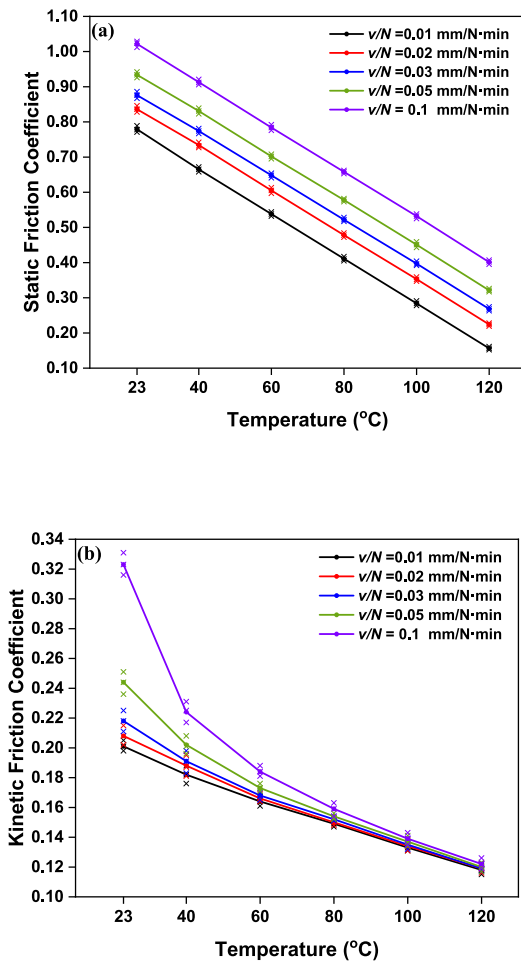


Fig. 17. Experimental friction coefficients under different temperatures: (a) Static; (b) Kinetic.

Once the resin flow occurs in a direction off-axis the fibre orientation at high temperatures, the fibres are more likely to move with the resin. The other reason for the uneven ply boundary displacement can be caused by the direct contact in some regions between the oriented fibres and aluminium sheet at high temperatures. When the normal force becomes

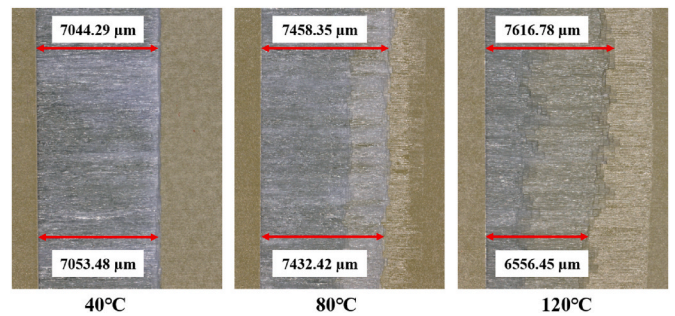


Fig. 18. Sliding surfaces after the friction test performed with different temperatures for 0°/0° interfaces– (× 12).

very high or the degree of cure for the epoxy prepreg increases, the sliding interface would be damaged as the viscosity increases and results in higher friction coefficients. Further research on laminate cut-outs after performing the friction test (Fig. 19) shows that the average thickness at the temperature of 40 °C is 303.7 μm, while it is 251.9 μm average at the temperature of 120 °C. The results imply that more resin flow at elevated temperature would lead to a distinct decrease in cross-section thickness.

As stated in the theoretical section of this paper, viscosity is another critical index on the Hersey number in the Stribeck-curve theory. A constant preheat time under various test temperatures was incorporated into the viscosity model. The relationships of friction coefficient and Hersey number at these test temperatures were made into a fitting curve with the average experimental results shown in Fig. 20. The result ignores the viscosity parameter in Hersey numbers for the static friction coefficient while a temperature compensation term [43,44] for both friction coefficients is considered to incorporate into the inter-ply friction model.

5. Development of inter-ply friction model

The inter-ply friction model for the kinetic friction is derived from the Stribeck curve theory investigation by fitting a curve to the results in Fig. 13(a),

$$\mu_k = 0.22 \cdot e^{27.25H} - 0.03 \tag{9}$$

where μ_k is the kinetic friction coefficient and H is the Hersey number.

It can be seen that an exponential fit represents the data well at room temperature and suggests that the range of values studied corresponds to the hydrodynamic lubrication domain in the Stribeck curve (Fig. 2).

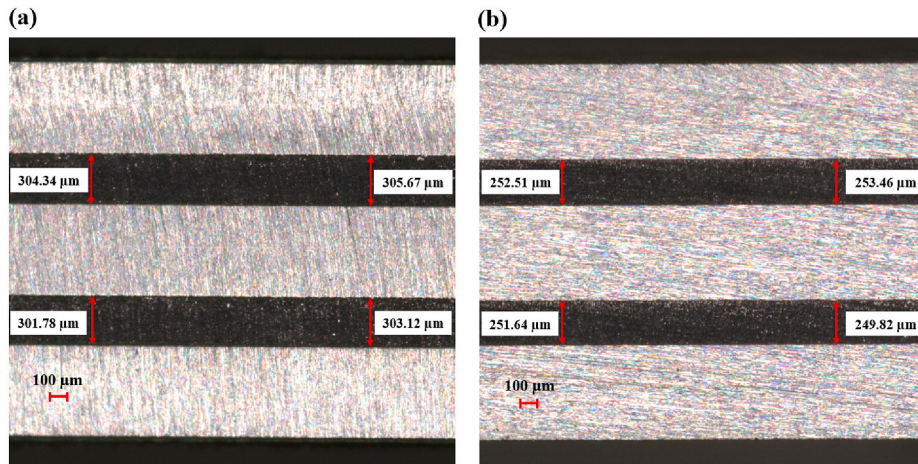


Fig. 19. Cross-section micrographs after friction test performed with a temperature of (a) 40 °C and (b) 120 °C – (× 80).

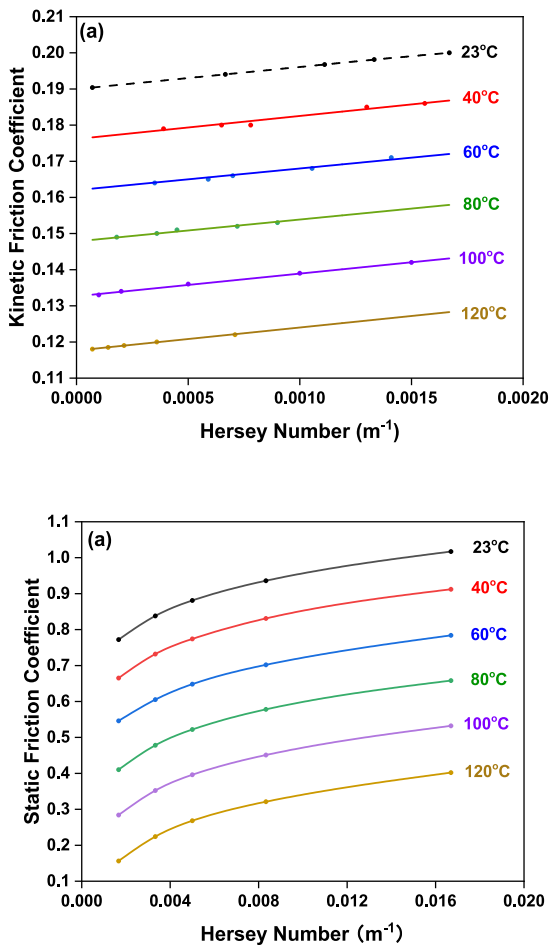


Fig. 20. Effect of test temperature on experimental friction coefficient and Hersey number: (a) Kinetic; (b) Static.

However, the trend for the fitting curve only corresponds with the experimental results at room temperature when the viscosity effect at different test temperatures is not considered. To account for the variations of temperature for the kinetic friction coefficient in the friction model, Gorczyca et al. [43] proposed a temperature shift term, S_{kk} ,

which can be added to the model,

$$\mu_k = (0.22 \cdot e^{27.25H} - 0.03) - S_{kk} \quad (10)$$

where S_{kk} is the shift term to compensate for the temperature effect. Based on the result obtained from Fig. 20(a), a linear fit can be matched to the test temperature versus kinetic friction data and the friction coefficient can be expressed as:

$$\mu_{kk} = -7.42 \times 10^{-4} \cdot T + 2.27 \times 10^{-1} \quad (11)$$

where μ_{kk} is the kinetic friction coefficient at the temperature T in °C. Then, the shift term for Eq. (10) is written which represents the difference between μ_{kk} at the baseline temperature (23 °C) and the actual test temperature,

$$S_{kk} = -7.42 \times 10^{-4} (T_B - T_A) \quad (12)$$

where T_A, T_B are the value of the actual temperature and baseline temperature in °C, respectively. Incorporating the result from Eq. (12) into Eq. (10) with the temperature difference $\Delta T = T_A - T_B$, the kinetic friction coefficient considering the investigated sliding effect is expressed as:

$$\mu_k = 0.22 \cdot e^{27.25 \frac{V}{N}} - 7.42 \times 10^{-4} \cdot \Delta T - 0.03 \quad (13)$$

where η, ν, N and ΔT are the processing parameters of resin viscosity, sliding velocity, normal force and temperature difference, respectively. From the Eq. (13), it can be concluded that the kinetic friction plots in the transition region between mixed and hydrodynamic lubrication can be fit into the Stribeck curve.

However, the fitting curve for static friction coefficient versus Hersey number (Fig. 13(b)) does not match with the Stribeck curve. The result found in Fig. 20(b) reveals that the viscosity parameter in the Hersey number has no contribution to establish a static friction model, while the shift term should be applied to compensate for temperature effect. Therefore, the static friction coefficient following a power-law fit at room temperature can be written as:

$$\mu_s = 5.02 \cdot \left(\frac{V}{N}\right)^{0.12} \quad (14)$$

where μ_s is the static friction coefficient, ν is the sliding velocity and N is the applied normal force. To compensate for test temperature effect on the static friction, a static shift term is added to the model again [43]. This shift term S_{ss} also corresponds to a linear fit according to Fig. 20(b) and the static friction coefficient at actual temperature, μ_{ss} , can be expressed as:

$$\mu_s = 5.02 \cdot \left(\frac{v}{N}\right)^{0.12} - S_{ss} \quad (15)$$

$$\mu_{ss} = -6.35 \times 10^{-3} \cdot T + 9.84 \times 10^{-1} \quad (16)$$

$$S_{ss} = -6.35 \times 10^{-3} (T_B - T_A) \quad (17)$$

where T_A , T_B are the value of the actual temperature and the baseline temperature in °C, respectively. Then, the static friction coefficient considering the investigated sliding effect can be written as,

$$\mu_s = 5.02 \cdot \left(\frac{v}{N}\right)^{0.12} - 6.35 \times 10^{-3} \cdot \Delta T \quad (18)$$

Here, the static friction coefficient is determined as a function of sliding velocity v , normal force N and temperature difference ΔT . This static friction model can be fit into a modified Coulomb friction model by combining Eq. (1) and Eq. (2) where $\mu = k \cdot N^{n-1}$ with a friction index $n = 0.88$. The modified friction model considers temperature effects and the friction constant k is also influenced by sliding velocity. It is known from the model that the test temperature has the largest influence on static friction, followed by the applied normal force and the sliding velocity. As a result, an inter-ply friction model considering the static and kinetic friction coefficients under different sliding parameters can be applied in process simulation.

6. Finite element model

The commercially available finite element package Abaqus/Explicit allows for the implementation of user-defined frictional behaviour via a subroutine. A finite element model of the experimental friction setup was run to validate the ability of the proposed friction model to replicate the response of the inter-ply friction test. This validation can give credibility that a finite element model of the forming simulation will correctly calculate friction based on normal forces, velocities and temperatures which may occur during the hot-pressing process. A finite element model of the inter-ply friction test shown in Fig. 21 consists of a top platen, a bottom platen and a laminate sample with surface to surface contact. Four node rigid shell elements were used to model the top and bottom platens, which assumed to be rigid bodies relative to the laminate. For the simulated fibre metal laminate, the aluminium sheet was modelled as deformable bodies using eight-node solid elements (C3D8R) and the glass fibre reinforced prepreg was created as deformable bodies with eight-node quadrilateral continuum shell elements (SC8R). The simulated laminate was represented in the composite layup module where all layers and their parameters such as orientation, thickness, material data and relative location were defined.

A normal force corresponding to the inter-ply friction characterisation experiments was applied on the fixed top and bottom platens in first step of the analysis. In the subsequent steps, the applied force was held constant and a velocity was prescribed in the pull-out direction on the middle aluminium sheet for a maximum distance of 20 mm. A static-kinetic exponential decay equation (Eq. (19)) was used to model the transition from static to kinetic friction under different sliding effects,

$$\mu = \mu_k + (\mu_s - \mu_k) \cdot e^{-\beta \dot{\gamma}} \quad (19)$$

where μ_s is the static friction coefficient μ_k is the kinetic friction coefficient, β is the decay constant and $\dot{\gamma}$ is the slip rate. The decay constant

defines the transition rate from zero velocity to the final velocity, and a decay constant of 0.16 is calculated to best-fit the experimental data points which can be used in the finite element models. The friction coefficient versus displacement curves from Abaqus/Explicit friction-test and experimental validation are plotted in Fig. 22 under some conditions. The model can capture a peak state as it is associated with the static friction and a steady sliding state for the kinetic friction. However, the static peak force and onset sliding displacement calculated from the model is lower than the experimental values and does not correspond to the experimental data. Because the kinetic friction coefficient is the dominating factor, the peak value is less important and can be fixed by a contact stiffness constant in the model. Therefore, the friction coefficient results indicate that the finite element model accurately accounts for the variations in sliding velocity, normal force and temperature to update the friction coefficient as a function of the test conditions. Through incorporating the inter-ply friction model into Abaqus/Explicit as a user-defined friction subroutine, an accurate hot-pressing simulation of thermoset based fibre metal laminates can be established.

7. Conclusion

The inter-ply friction coefficient at the metal-prepreg interfaces for glass-fibre reinforced aluminium laminate (GLARE) under different sliding parameters has been measured using a designed friction-test apparatus. The influenced sliding parameters were normal force, sliding velocity, fibre orientation, resin viscosity coupled with the temperature. Friction coefficient outcomes are further studied by the sliding displacement and cross-section thickness measurements. The sliding parameters which would decrease the friction coefficients are obtained and an inter-ply friction model based on the experimental result is incorporated into Abaqus/Explicit as a user-defined friction subroutine. The main achievements are:

- The static friction coefficient increases with the increasing sliding velocity and decreases with the increasing normal force, while the kinetic friction coefficient drops with the increasing normal force at

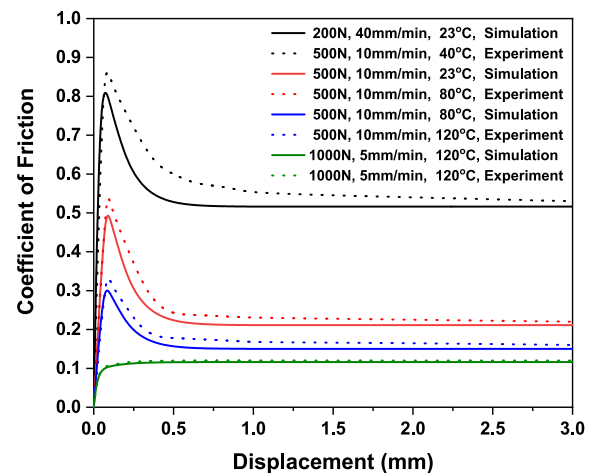


Fig. 22. Friction coefficient versus displacement curves from simulation model and experimental validation.

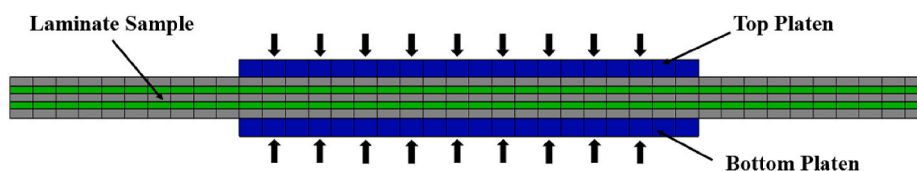


Fig. 21. Finite element model of the inter-ply friction test of the pre-stacked laminates.

various sliding velocities before reaching a minimum value and plateau. Also, the static friction coefficient drops quasi-linear with the increase of test temperature. In contrast, the kinetic friction coefficient gradually converges at elevated temperature due the decreased of resin viscosity. Combining the effect of the sliding velocity and normal force has a small influence on kinetic friction when the temperature becomes higher.

- The fibre orientation has limited influence on the coefficient of static friction while the fibre oriented at $45^\circ/45^\circ$ exhibits the highest kinetic friction coefficient and the $0^\circ/0^\circ$ interfaces show a lower friction coefficient compared with $90^\circ/90^\circ$ interfaces under the same conditions. Inter-ply sliding dominates the evolution of the friction coefficient but the intra-ply shear behavior within the prepreg also affects the friction. In addition, the decreasing viscosity at elevated temperature has a significant influence on both inter-ply sliding and intra-ply shear behaviours.
- The kinetic friction for various combinations of sliding effects results in a relationship similar to the Stribeck curve, which plots in the transition region between mixed and hydrodynamic lubrication. The static friction coefficient versus Hersey number does not match the trend in Stribeck-curve theory but obeys a modified Coulomb type of friction where resin viscosity has limited influence.
- A static-kinetic exponential decay equation in Abaqus/Explicit was used to model the transition from static to kinetic friction. The kinetic friction was validated to be the dominating factor in the finite element model, and the friction coefficients obtained from the simulations correlate well with the experimental results.

Author contribution

All authors contribute substantially to the paper. Shichen Liu (first author) carried out the experimental setup, analysis of the experimental data and manuscript writing; Jos Sinke and Clemens Dransfeld provide the ideas for experimental design, knowledge of resin rheology and help to revise the manuscript. All authors read and approved the final manuscript.

Declaration of competing interest

The authors declare that they have no known competing financial interests or personal relationships that could have appeared to influence the work reported in this paper.

Acknowledgements

The authors would like to thank the financial supports of China Scholarship Council (No.201906040174).

Appendix A. Supplementary data

Supplementary data to this article can be found online at <https://doi.org/10.1016/j.compositesb.2021.109400>.

References

- [1] Asundi A, Choi AYN. Fiber metal laminates: an advanced material for future aircraft. *J Mater Process Technol* 1997;63(1–3):384–94.
- [2] Sinmazçelik T, Avcu E, Bora MÖ, Çoban O. A review: fibre metal laminates, background, bonding types and applied test methods. *Mater Des* 2011;32(7):3671–85.
- [3] Wang RM, Zheng SR, Zheng YP. Matrix materials. *Polym Matrix Compos Technol* 2011;101–548.
- [4] Khan MA, Reynolds N, Williams G, Kendall KN. Processing of thermoset prepregs for high-volume applications and their numerical analysis using superimposed finite elements. *Compos Struct* 2015;131:917–26.
- [5] Pasco C. Characterisation of the thermoset prepreg compression moulding process. *ACCE SPE Conf* 2016;September.
- [6] Sinke J. Manufacturing of GLARE parts and structures. *Appl Compos Mater* 2003;10(4–5):293–305.
- [7] Sinke J. Feasibility of tailoring of press formed thermoplastic composite parts. *AIP Conf Proc*. May; 2018.
- [8] Ersoy N, Potter K, Wisnom MR, Clegg MJ. An experimental method to study the frictional processes during composites manufacturing. *Compos Part A Appl Sci Manuf* 2005;36(11):1536–44.
- [9] Fetfatsidis KA, Jauffrès D, Sherwood JA, Chen J. Characterization of the tool/fabric and fabric/fabric friction for woven-fabric composites during the thermostamping process. *Int J Material Form* 2013;6(2):209–21.
- [10] Najjar W, Pupin C, Legrand X, Boude S, Soulat D, Dal Santo P. Analysis of frictional behaviour of carbon dry woven reinforcement. *J Reinforc Plast Compos* 2014;33(11):1037–47.
- [11] Allaoui S, Cellard C, Hivet G. Effect of inter-ply sliding on the quality of multilayer interlock dry fabric preforms. *Compos Part A Appl Sci Manuf* 2015;68:336–45.
- [12] Pasco C, Khan M, Gupta J, Kendall K. Experimental investigation on interply friction properties of thermoset prepreg systems. *J Compos Mater* 2019;53(2):227–43.
- [13] Martin CJ, Seferis JC, Wilhelm MA. Frictional resistance of thermoset prepregs and its influence on honeycomb composite processing. *Compos Part A Appl Sci Manuf* 1996;27(10):943–51.
- [14] Åkermo M, Larberg YR, Sjölander J, Hallander P. Influence of interply friction on the forming of stacked UD prepreg. *ICCM Int Conf Compos Mater*. July 2013: 919–28.
- [15] Smolnicki M, Stabla P. Finite element method analysis of fibre-metal laminates considering different approaches to material model. *SN Appl Sci* 2019;1(5):1–7.
- [16] Soltani P, Keikhosravi M, Oskouei RH, Soutis C. Studying the tensile behaviour of GLARE laminates: a finite element modelling approach. *Appl Compos Mater* 2011;18(4):271–82.
- [17] Zal V, Moslemi Naeini H, Sinke J, Bahramian AR, Abouhamzeh M, Benedictus R. A new procedure for Finite Element simulation of forming process of non-homogeneous composite laminates and FMLs. *Compos Struct* 2017;163:444–53.
- [18] Boisse P, Buet K, Gasser A, Launay J. Meso/macro-mechanical behaviour of textile reinforcements for thin composites. *Compos Sci Technol* 2001;61(3):395–401.
- [19] Boisse P, Hamila N, Helenon F, Hagege B, Cao J. Different approaches for woven composite reinforcement forming simulation. *Int J Material Form* 2008;1(1):21–9.
- [20] Jauffrès D, Sherwood JA, Morris CD, Chen J. Discrete mesoscopic modeling for the simulation of woven-fabric reinforcement forming. *Int J Material Form* 2010;3:1205–16.
- [21] Mosse L, Compston P, Cantwell WJ, Cardew-Hall M, Kalyanasundaram S. The development of a finite element model for simulating the stamp forming of fibre-metal laminates. *Compos Struct* 2006;75(1–4):298–304.
- [22] ASTM D 1894-1995. Standard test method for static and kinetic coefficients of friction of plastic film and sheeting. *Annu. B. ASTM Standard International*.
- [23] Maldonado JE. Coefficient of friction measurements for plastics against metals as a function of normal force. In: *Special areas proceedings of the 56th annual technical conference, ANTEC*. Part. vol. 3; 1998. p. 3431.
- [24] Lussier D, Chow S. Shear and friction response of commingled glass-polypropylene fabrics during stamping. *Proceedings for the American society for composites 16th technical conference*. 2001. VA.
- [25] Chow S. Frictional interaction between blank holder and fabric in stamping of woven thermoplastic composites. Master thesis. Department of Mechanical Engineering, University of Massachusetts Lowell; 2002.
- [26] Ajayi JO. Fabric smoothness, friction and handle. *Textil Res J* 1992;62:52–9.
- [27] Ajayi JO. Effect of fabric structure on frictional properties. *Textil Res J* 1992;62:87–93.
- [28] Stachowiak GW, Batchelor AW. *Engineering tribology*. Butterworth-Heinemann; 2000.
- [29] Wilks CE. Characterisation of the tool/ply interface during forming. PhD thesis. UK: School of Mechanical, Materials, Manufacturing Engineering and Management University of Nottingham; 1999.
- [30] Clifford M, Long A, DeLuca P. Forming of engineering prepregs and reinforced thermoplastics. *Global symposium on innovations in materials, processing and manufacturing: composite processing*. February 11– 2001;15.
- [31] Gelinck ER, Schipper DJ. Calculation of Stribeck curves for line contacts. *Tribol Int* 2000;33:175–81.
- [32] Gorczyca JL, Sherwood JA, Liu L, Chen J. Modeling of friction and shear in thermostamping of composites - Part I. *J Compos Mater* 2004;38(21):1911–29.
- [33] Larberg YR, Åkermo M. On the interply friction of different generations of carbon/epoxy prepreg systems. *Compos Part A Appl Sci Manuf* 2011;42(9):1067–74.
- [34] Baran I, Akkerman R, Hattel JH. Material characterisation of a polyester resin system for the pultrusion process. *Compos B Eng* 2014;64:194–201.
- [35] Geissberger R, Maldonado J, Bahamonde N, Keller A, Dransfeld C, Masania K. Rheological modelling of thermoset composite processing. *Compos B Eng* 2017;124:182–9.
- [36] Sun L. Thermal rheological analysis of cure process of epoxy prepreg. *Dep Chem Eng* 2002;PhD:127.
- [37] Solvay Adhesive Materials. *Technical Data Sheet FM- 94 Film Adhesive*. <https://www.solvay.com/en/product/fm-94#product-documents>.
- [38] Li H, Lu Y, Han Z, et al. The shotpeen forming of fiber metal laminates based on the aluminum-lithium alloy: deformation characteristics. *Compos B Eng* 2019;158:279–85.
- [39] Hua X, Li H, Lu Y, Chen Y, Qiu L, Tao J. Interlaminar fracture toughness of GLARE laminates based on asymmetric double cantilever beam (ADCB). *Compos B Eng* 2019;163:175–84.
- [40] ASTM International. D3528-96 standard test method for strength properties of double lap shear adhesive joints by Am Soc Test Mater 2016;96.

- [41] Abouhamzeh M, Sinke J, Jansen KMB, Benedictus R. Kinetic and thermo-viscoelastic characterisation of the epoxy adhesive in GLARE. *Compos Struct* 2015; 124:19–28.
- [42] Abouhamzeh M, Sinke J, Jansen KMB, Benedictus R. A new procedure for thermo-viscoelastic modelling of composites with general orthotropy and geometry. *Compos Struct* 2015;133:871–7.
- [43] Gorczyca-Cole JL, Sherwood JA, Chen J. A friction model for thermostamping commingled glass-polypropylene woven fabrics. *Compos Part A Appl Sci Manuf* 2007;38(2):393–406.
- [44] Sachs U, Akkerman R, Fetfatsidis K, et al. Characterization of the dynamic friction of woven fabrics: experimental methods and benchmark results. *Compos Part A Appl Sci Manuf* 2014;67:289–98.